FREEZE-FRACTURE STUDIES OF THE DEVELOPING CELL SURFACE

I. The Plasmalemma of the Corneal Fibroblast

DAVID L. HASTY and ELIZABETH D. HAY

From the Department of Anatomy, Harvard Medical School, Boston, Massachusetts 02115

ABSTRACT

The freeze-fracture technique was used to study changes in the corneal fibroblast cell membrane during morphogenesis in chick embryos. Fibroblasts migrate into the acellular primary corneal stroma on day 6 of embryogenesis, moving between the orthogonal layers of collagen fibrils which serve as their substratum. Morphometric analysis of the intramembrane particles (IMP) reveals their concentration on the P face to decrease from 756 to 534/μm^2 from day 6 to day 14. After day 14, fibroblast migration and cell division cease and the stroma condenses due to dehydration, so that by day 18 all of the layers of fibroblasts are extremely flattened and the cornea has taken on its mature, transparent form. The cell membranes of the terminally differentiated, highly compacted fibroblasts are rich in IMP (1,300/μm^2, P face). In seeking to relate the particle increase to cell differentiation, we analyzed synthetic events taking place at this time, but no correlation with $^{25}SO_4$ or proline-^3H incorporation was found. The event which seems best correlated with the doubling of P face particles between days 15 and 18 is the dehydration and condensation of the stroma, an event which is associated with cessation of both cell division and migration. Thyroxine stimulates premature condensation of the stroma, whereas thiouracil delays condensation, but neither of these treatments affects IMP concentration. Interestingly, IMP concentration on the filopodia of migrating fibroblasts is similar to that on the cell bodies, suggesting that the new membrane has the same composition as the pre-existing membrane. Observations are also presented on tight and gap junctions between fibroblasts and on the relation of extracellular matrix to the outer etched surface of the fibroblast plasmalemma.

The first event in avian corneal morphogenesis is the laying down of an acellular stroma of orthogonal layers of collagen fibrils embedded in glycosaminoglycan (GAG);[1] both the collagen and GAG are products of the epithelium (14, 31). Subsequently, the endothelium migrates into place under the stroma and secretes hyaluronate into its interstices, bringing about, directly or indirectly, a remarkable swelling of the matrix (21, 52, 55). The neural crest cells which will become corneal fibroblasts (24) migrate into the acellular, primary corneal stroma on day 6 of embryogenesis in the chick, moving between the orthogonal layers of

[1] Abbreviations used in this paper are: GAG, glycosaminoglycan; ECM, extracellular matrix; IMP, intramembranous particle; CAM, chorioallantoic membrane; ES, extracellular cell surface; SR, sarcoplasmic reticulum.

collagen fibrils that seem to serve as their substratum (4, 21).

From the time of their appearance at day 6, the presumptive corneal fibroblasts actively migrate and proliferate in the stroma, so that by day 14 only the subepithelial stroma remains uninvaded. During the period between days 6 and 14, these relatively undifferentiated mesenchymal cells acquire abundant secretory organelles (endoplasmic reticulum, Golgi complexes) and begin to add collagen and GAG to that present in the original stroma (21). After day 14, fibroblast migration and cell division cease and the stroma condenses under the influence of the thyroid hormone that now appears in the embryo. By day 18, all of the layers of fibroblasts are extremely flattened and the cornea has taken on its mature, transparent form (12, 13, 29). Thus, there are at least three relatively discrete but overlapping phases in corneal fibroblast differentiation: one in which the major activity of the cells is migration and proliferation, a second when the cells settle down to the business of secreting extracellular matrix (ECM), and a third when fibroblast proliferation ceases and the cornea condenses and becomes transparent.

We have used the freeze-fracture technique to study developmental changes in fibroblast plasmalemma ultrastructure during the three phases of cytodifferentiation described above. It is now generally accepted that this technique offers a unique view of membrane ultrastructure by splitting the lipid bilayer along its hydrophobic interior (40, 51). Most information to date indicates that the globular, particulate units which freeze-fracture reveals embedded in the cleaved membrane are proteins or lipoproteins and that the flattened areas surrounding these intramembranous particles (IMP) represent the "half-bilayer" lipid domain (8, 22, 28, 47). Morphologic alterations of particulate and lipid domains occur in different functional states (37, 49, 53). Moreover, intra- and inter-membrane interactions of protein and lipid components can be expressed in morphologically recognizable forms, such as tight and gap junctions (9, 17). Thus, it seemed reasonable to expect that distinct morphologic changes in the fibroblast plasmalemma might be detected during embryogenesis.

In this paper, we describe the general appearance of the corneal fibroblast and surrounding stroma in freeze-fracture replicas and the changes that occur in fibroblast plasmalemma ultrastructure during corneal morphogenesis. In addition, biochemical studies of matrix synthesis and studies employing thiouracil and thyroxine are reported which were performed to find out whether the increase that was observed in IMP number in the third phase of corneal development was related to the level of synthesis of GAG and collagen or to the initiation of thyroid function and accompanying stromal condensation.

MATERIALS AND METHODS

Electron Microscopy

Corneas from White Leghorn chicken embryos (SPAFAS, Norwich, Conn.) were dissected free of extraneous material and fixed by immersion in a sodium cacodylate buffer (0.1 M, pH 7.4) containing paraformaldehyde (1%) and glutaraldehyde (2.5%). Tissue which would subsequently be used for freeze-fracture was fixed for approximately 30–60 min at room temperature, washed several times in buffer, and then glycerinated (20% glycerol, 0.1 M cacodylate buffer, 0.4% $CaCl_2$, pH 7.4) for approximately 1 h. Care was taken not to overglycerinate the tissue. After glycerination, pieces of cornea were mounted on paper disks and frozen immediately in liquid nitrogen-cooled Freon 22. The tissue was fractured in a Balzers apparatus (Balzers High Vacuum Corp., Santa Ana, Calif.) at −115°C. The platinum-carbon replicas were left in 100% methanol overnight and then cleaned by floating over a commercial bleach. For etching, fixed specimens were frozen in distilled water, fractured at −108°C and etched for 30–60 seconds.

Tissue to be used for thin sectioning was fixed in formaldehyde-glutaraldehyde for 1–2 h at room temperature, followed by fixation in 1.5% OsO_4 for 1 h at 4°C. The tissue was stained en bloc with 1% uranyl acetate, dehydrated and embedded in Epon or Araldite. Before examination in the electron microscope, sections were stained with lead citrate.

Quantitation of Plasmalemma IMP Size and Concentration

Micrographs of the flat areas of replicas to be used for counting IMP were consistently taken at an initial magnification of ×20, 000. The accuracy of this magnification was checked from time to time with a grating replica standard (E. F. Fullam Co., Schenectady, N.Y.). These negatives were printed at a final magnification of 240,000 for measuring particle size and ×50,000 for counting particle number.

A standard morphometry grid was used to insure a random count of the discrete particles, 7–12 nm in diameter, lying within the fractured plasmalemma. An average of the numbers obtained in this manner was used to calculate the number of particles per square micrometer

on the original surface. 8–10 cells and an area of 2–4 μm^2 per cell were counted for each group. All of our observations indicated a uniform distribution of IMP over the entire plasmalemma of each cell, except in regions of intercellular junctions.

The P face[2] IMP diameter was measured as the width of the shadow cap perpendicular to the direction of shadowing, using a dissecting microscope fitted with a calibrating grid to view the micrographs. 75–100 particles were measured on each four cells at both 6 and 19 days of incubation. Although IMP size measured from freeze-fracture replicas obviously bears no direct relationship to the actual size of the shadowed membrane proteins (33), relative changes in particle size classes measured in this way probably do reflect relative changes in protein size classes.

Cytoplasmic area and membrane perimeter of 14- and 19-day fibroblasts were measured by a standard two-dimensional morphometric test. Electron micrographs were taken randomly of sections from three tissue blocks of both age groups. Negatives were enlarged to a final magnification of 15,000 for counting. Plasmalemma perimeter length and cytoplasmic area were calculated from membrane intersections and cytoplasm hits, respectively.

Measurements of Collagen and GAG Production

The changes in synthetic activity of corneal fibroblasts were surveyed during the period of stromal condensation, from day 14 to day 19. Previous studies have demonstrated that there is no increase in the number of cells in the cornea from day 14 through hatching (10, 11). Therefore, the synthetic activity of older corneas expressed in counts per minute per cornea can be compared directly to the synthetic activity of 14-day corneas similarly expressed (relative incorporation, Fig. 18).

Corneas were dissected free of extraneous material and treated with 0.04% EDTA in calcium and magnesium-free Hanks' salt solution to allow removal of the epithelium and endothelium. Synthetic activity of the remaining stroma was monitored by analysis of [^{3}H]glucosamine and [^{3}H]proline incorporation (for GAG and collagen, respectively) during a 4-h incubation at 37°C in Ham's F12 culture medium with 10% fetal calf serum and the appropriate isotope. The details of these methods have been reported previously (32). Briefly, newly synthesized GAG was measured as radioactivity in cetylpyridinium chloride-precipitable material and collagen was measured as radioactivity in hot trichloroacetic acid-extractable material.

[2] The outer aspect of the inner leaflet of the bilayer which borders the cytoplasmic compartment will be designated the P face, while the inner aspect of the outer leaflet of the bilayer will be called the E face (7).

Thyroxine and Thiouracil Treatment

Embryos were treated with throxine at day 11 or thiouracil at day 9 and incubated until the age of 13 or 17 days, respectively. The sodium salt of thyroxine (Sigma Chemical Co., St. Louis, Mo.) was administered at a dosage of 15 μg per 0.1 ml and thiouracil (Nutritional Biochemical Corp., Cleveland, Ohio) at a dosage of 10 mg per 0.1 ml. Eggs were candled and a small hole was chipped in the shell over a well vascularized area of the chorioallantoic membrane (CAM). The solutions were applied as a suspension in 0.1 ml of 0.9% saline directly onto the CAM.

RESULTS

On the 6th day of avian embryogenesis, at Hamburger-Hamilton stage 27–28 (18), the presumptive corneal fibroblasts invade the posterior zone of the acellular corneal stroma near its endothelial border; subsequently, fibroblasts move into the anterior stroma to within a few microns of the overlying epithelial layer (Fig. 1). These mesenchymal cells are elongate and somewhat oval in shape while migrating, with lamellipodia and filopodia extending from the cell body (4, 21). In section, their attenuated profiles are seen to undulate to follow the architecture of the stromal collagen layers. Dividing cells tend to have a rounded shape and they extend numerous filopodia during anaphase (4). The fibroblasts rapidly increase in number during the next few days by continued inward migration of cells from the corneal periphery and by cell division within the cornea, so that they come to occupy most of the stroma by stage 35 (9 days, Fig. 1).

Beginning on about day 14, when the stroma starts to condense, the layers of collagen bundles become tightly packed and the fibroblasts very flattened in shape. The stromal condensation and flattening of the fibroblast cell shape begin in the layers closest to the endothelium (15 days, Fig. 1). Concomitant with the flattening of the cell body, both the filopodia and the cell body become oriented in the plane of the collagen plys (compare Fig. 2, *a* and *b*). Secretory organelles remain well developed (21) and the synthesis of extracellular matrix by these cells continues during this period, declining only after the completion of condensation at 18–19 days (10, 11).

General Observations on Freeze-Fractured Corneas

Pieces of cornea were mounted so that the knife, and thus the plane of fracture, passed

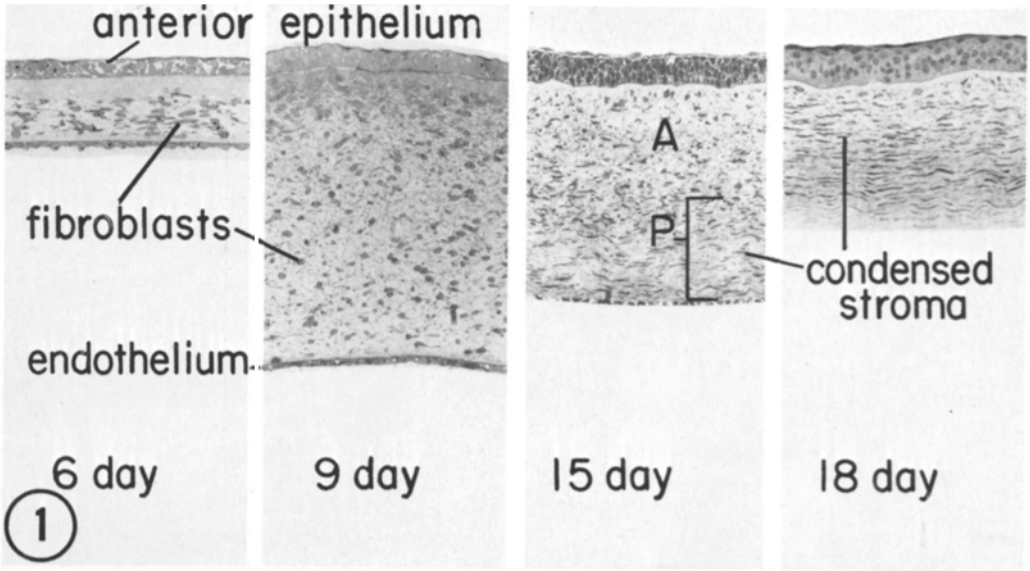

FIGURE 1 Light micrographs of sections through developing corneas at different ages. At 6 days, the fibroblasts have just begun to invade the collagenous primary stroma produced by the anterior epithelium. Between 6 days and 9 days, the number of fibroblasts in the stroma increases by proliferation and by continued inward migration of mesenchymal cells into the stroma. The width of the stroma continues to increase between 9 and 12 days due to both the number of cells and the collagen and GAG these cells produce. Cell proliferation ceases, between day 12 and day 14, and stromal condensation begins in the juxtaendothelial region. By 15 days, the posterior stroma (*P*) is condensed and the fibroblasts are flattened in that area, whereas the anterior stroma (*A*) is not yet condensed. The process continues until by 18 or 19 days the entire cornea is condensed and the cornea is transparent. × 216.

roughly parallel to the layers of collagen in the stroma. Since the fibroblasts lie between the collagenous lamellae, they are cleaved along the plane of their flattened long axis (Fig. 3). Due to the elongate shape of these cells, fractures can pass along their plasmalemma for considerable distances before breaking through the cytoplasmic compartment or into the extracellular space. Most fractures reveal only a small part of the surface of each fibroblast, however, and it is rare that one observes a cell membrane almost in its entirety, as in Fig. 3. In this fortunate plane of fracture, one may see a large, flat, branching lamellipodium (*la*, Fig. 3) and several narrow filopodia extending from the same cell body. Large (100–200 nm) pits are seen on the P face of fibroblasts (circular inset, Fig. 3). These pits probably represent exo- or endocytotic phenomena (15).

Since epithelia are sheets of contiguous cells having apical, basal, and lateral surfaces, fractures through the anterior corneal epithelium or the posterior endothelium usually reveal one or more of these distinctive surfaces and the cytoplasmic compartment of several cells. Fractures through the basal plasmalemma of either anterior or posterior epithelium reveal a jigsaw puzzle-like arrangement of contiguous cells. Typical junctional complexes (tight junctions, desmosomes, and gap junctions) are found on the lateral plasmalemma fracture faces of the anterior epithelial cells, but are not conspicuous in the embryonic endothelium.

In the description below of corneal fibroblasts, the fine structure of the ECM and outer (etched) cell surface as viewed in freeze-fractured specimens will first be considered briefly. The cleaved membrane of cell processes and intercellular junctions of fibroblasts will be described next. Then, we shall turn our attention to the main topic of this paper, the changes which take place in IMP during the development of the corneal fibroblasts.

Extracellular Matrix

Bundles of collagen are easily identified in the extracellular space. Individual fibrils often are not fractured; they seem to pull away from the fracture surface before they are torn apart. Their stems cast unusually long shadows across the rep-

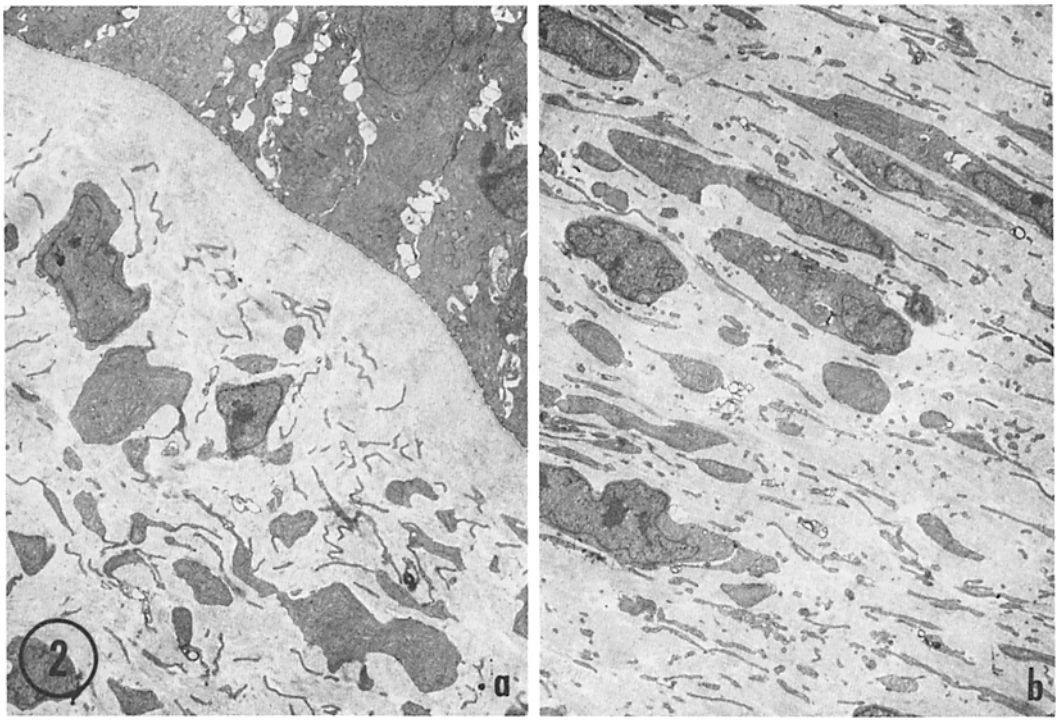

FIGURE 2 Electron micrographs of sections through the anterior (2*a*) and posterior (2*b*) portions of the corneal stroma of a 15-day chick embryo. The fibroblasts in the uncondensed anterior stroma (2*a*) remain rounded or elongate in shape, whereas these in the condensed posterior stroma are flattened (2*b*). Numerous filopodia can be seen in both micrographs. The anterior corneal epithelium appears across the upper right of 2*a*. × 7,000.

lica (arrow, Fig. 3). With the subsequent reduction of extracellular fluid, the bundles of collagen fibrils surrounding the fibroblasts gradually become sheets that occupy almost the entire extracellular space (Fig. 4*a*). Fractured fibrils show either a helical (Fig. 4*b*) or cross-banded (Fig. 4*c*) pattern (44).

Surrounding the fibrils, granular deposits are arranged in rows parallel to the long axis of the fibrils or at right angles to them (arrows, Fig. 4*a*). This interfibrillar material consists of particles 10 nm in diameter which probably correspond to the ruthenium red-staining glycosaminoglycan particles that are seen in the matrix in thin sections of fixed specimens (20, 25, 32, 34, 55).

The relationship of ECM to the fibroblast cell surface can be appreciated from micrographs of etched corneas. Etching reveals that the extracellular cell surface (*ES*) is relatively smooth in appearance as compared to the fractured membrane faces. There are, however, knobs of material (25–30 nm diameter) studding the surface, which sometimes contain a central raised area 8–10 nm in diameter (arrows, Fig. 5). It is possible to detect filaments (5–10 nm in diameter) extending from these knobs either into the extracellular space or onto the surface of a collagen fibril (Figs. 5–8). Etching causes the filaments to stand out in the extracellular space also and reveals that they overlap or interconnect to form a "chicken-wire" arrangement as seen in a two dimensional plane (Figs. 7 and 8). The pattern of eutectic artefact, which is sometimes revealed by etching, vaguely resembles that of these filaments, but the morphology of eutectic is quite distinct and not easily mistaken for the filaments illustrated in Fig. 8. The composition of these extracellular filaments is presently unknown, but they may be comparable to the minute filaments which have been previously reported in the ECM and on the cell surface in sections of ruthenium red-fixed specimens (20, 25, 34, 55).

Cell Processes

We have been able to identify cell processes of various sizes in freeze-fracture replicas of older

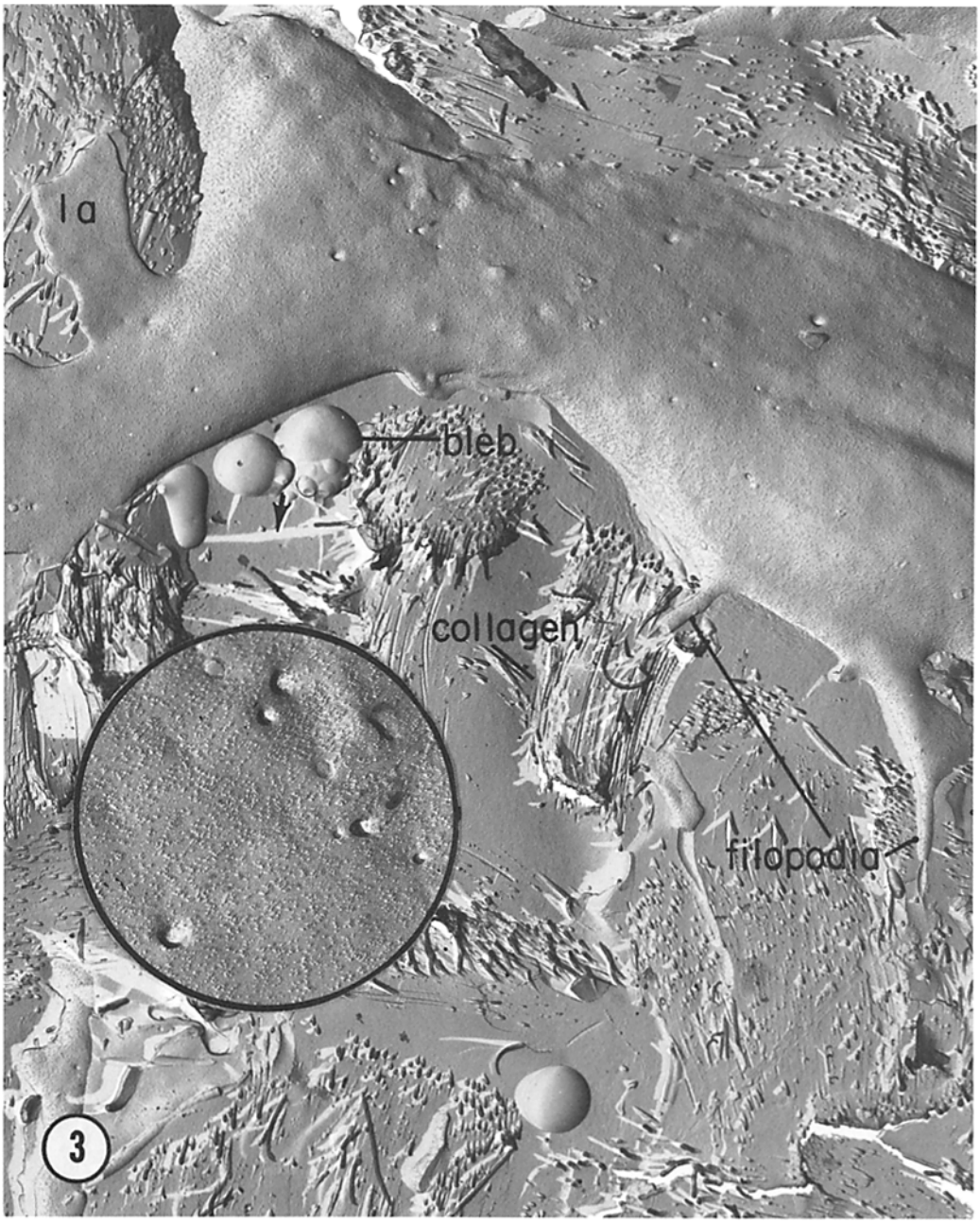

FIGURE 3 An electron micrograph of a freeze-fracture replica through the anterior corneal stroma of a 15-day embryo. The fracture revealed almost the entirety of this fibroblast. The large, flat lamellipodium (*la*) and narrow filopodia can be easily identified extending from the cell body. Collagen bundles are seen in the extracellular space. Some of the fibrils are not fractured and they break as they are pulled out and away from the surface. Such a fibril stem may cast a long shadow (arrow) across the replica. Large (100–200 nm) pits, probably representing exo- or endocytotic events, are seen on the P face of this fractured cell (see inset also). IMP cover the fractured P face. × 14,000. Inset, × 33,000.

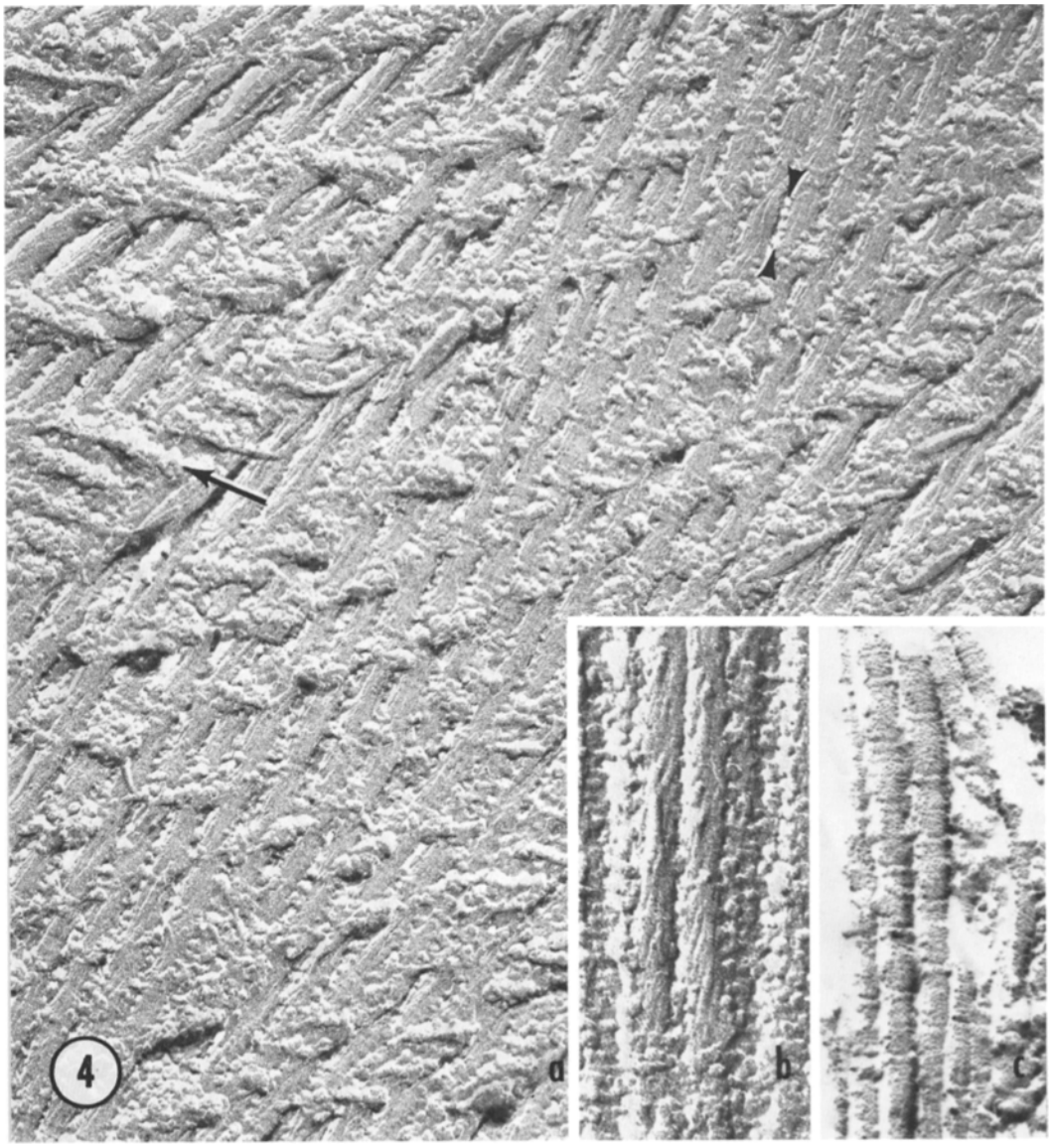

FIGURE 4 Electron micrographs of the ECM surrounding adult corneal fibroblasts. The ECM before condensation in the embryo consists of widely separated bundles of collagen fibrils, but as condensation is completed, and throughout adulthood, the ECM takes the form of continuous sheets of collagen. The collagen fibrils are packed very closely, separated by a granular substance which is arranged in rows either parallel to the long axis of the fibrils (arrowheads, 4*a*) or at right angles to them (arrow, 4 a). Fractured fibrils can show either a helical (4*b*) or cross-banded (4*c*) pattern. *a*, × 114,000; *b*, × 147,000; *c*, × 128,000.

corneas containing stationary fibroblasts (Figs. 3 and 9) as well as early corneas containing actively migrating fibroblasts (Figs. 10 and 11). These cell processes (filopodia, lamellipodia) are seen either as they branch off the cell body or at some distance from the cell body, but rarely does their entire length appear in one fracture. They usually run parallel to the collagen bundles rather than at angles to the direction of the fibrils. Filopodia (100–300 nm in diameter) and lamellipodia (>400 nm) of the migrating cells probably function to explore the new terrain for desirable direc-

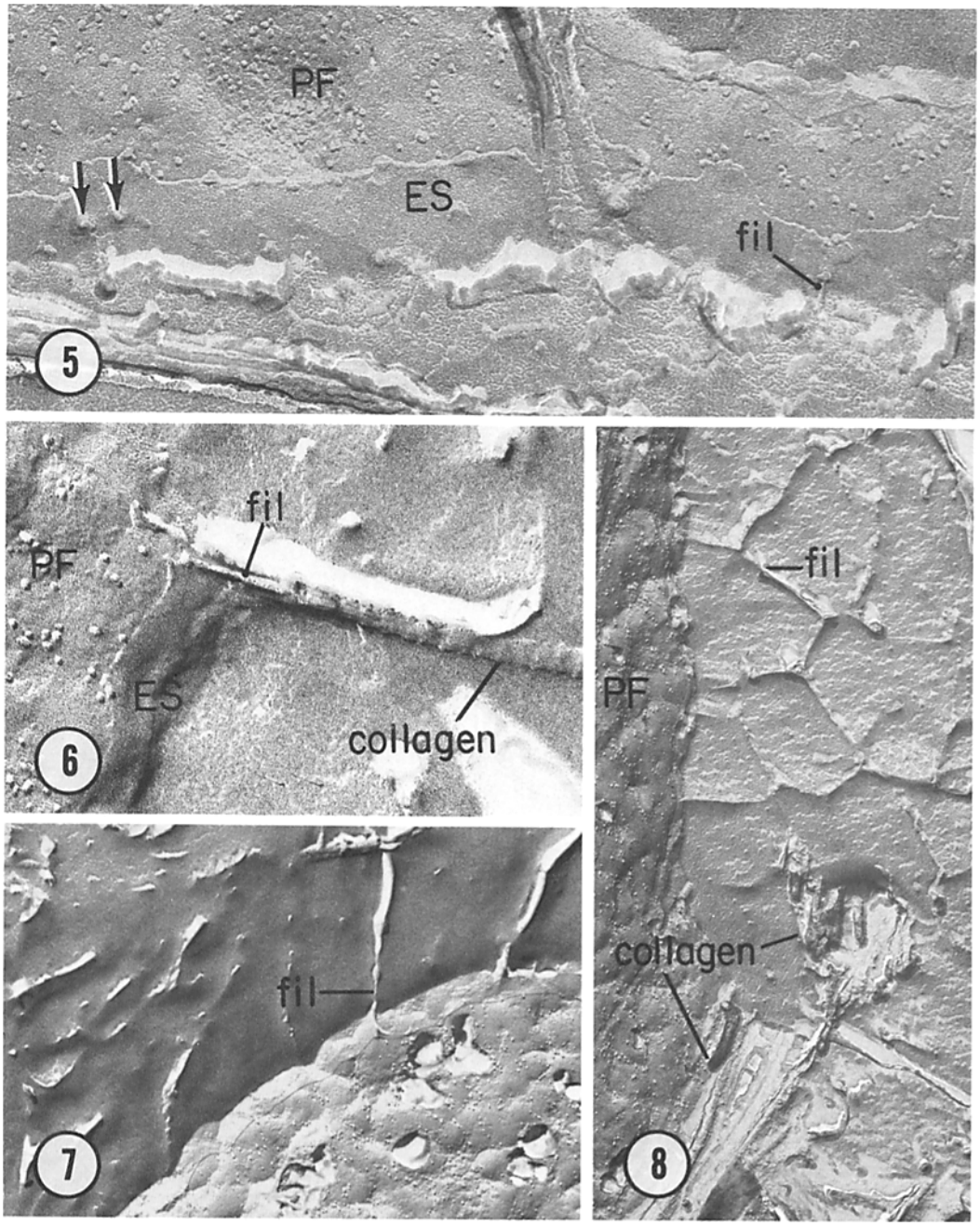

FIGURES 5–8 Electron micrographs of freeze-etched 9-day corneas demonstrating the relationship of the ECM to the cell surface. The etched, external surface (*ES*) of the corneal fibroblast is relatively smooth, compared to the particle-studded, fractured P face (*PF*). One does, however, observe knobs of material on the ES (arrows, Fig. 5), sometimes giving rise to small filaments (*fil*) 5–10 nm in diameter that may extend to a collagen fibril (Fig. 6). Etching causes the filaments to stand out in the extracellular space (*fil*, Figs. 7 and 8), and suggests that they overlap or interconnect to form a "chicken-wire" arrangement (Fig. 8). Fig. 8 demonstrates the relationship of the cells, filaments, and bundles of etched collagen fibrils. Fig. 5, × 98,000; Fig. 6, × 135,000; Fig. 7, × 36,000; Fig. 8, × 45,000.

tions for movement (2, 4). In both young and old corneas, they form attachments to the substratum and to adjacent cells (2, 4).

We have especially examined filopodia to try to determine whether or not there are morphological specializations of the plasmalemma which might be involved in cell-substrate contact. To date, we have seen no unique membrane architecture in young or older corneas which would document the contact of the filopodium with the ECM. Fractures revealing the P or E face of the plasmalemma of cell processes have always shown the number and arrangement of IMP to be roughly similar to that of the cell body (Figs. 3, 9–11).

Interestingly, particle-free membrane blebs occur as a rather common feature in fracture replicas of the corneal stroma, particularly in younger specimens (*Bleb*, Fig. 3). These structures resemble the cytoplasm-free membrane vesicles very commonly seen in thin sections of the developing

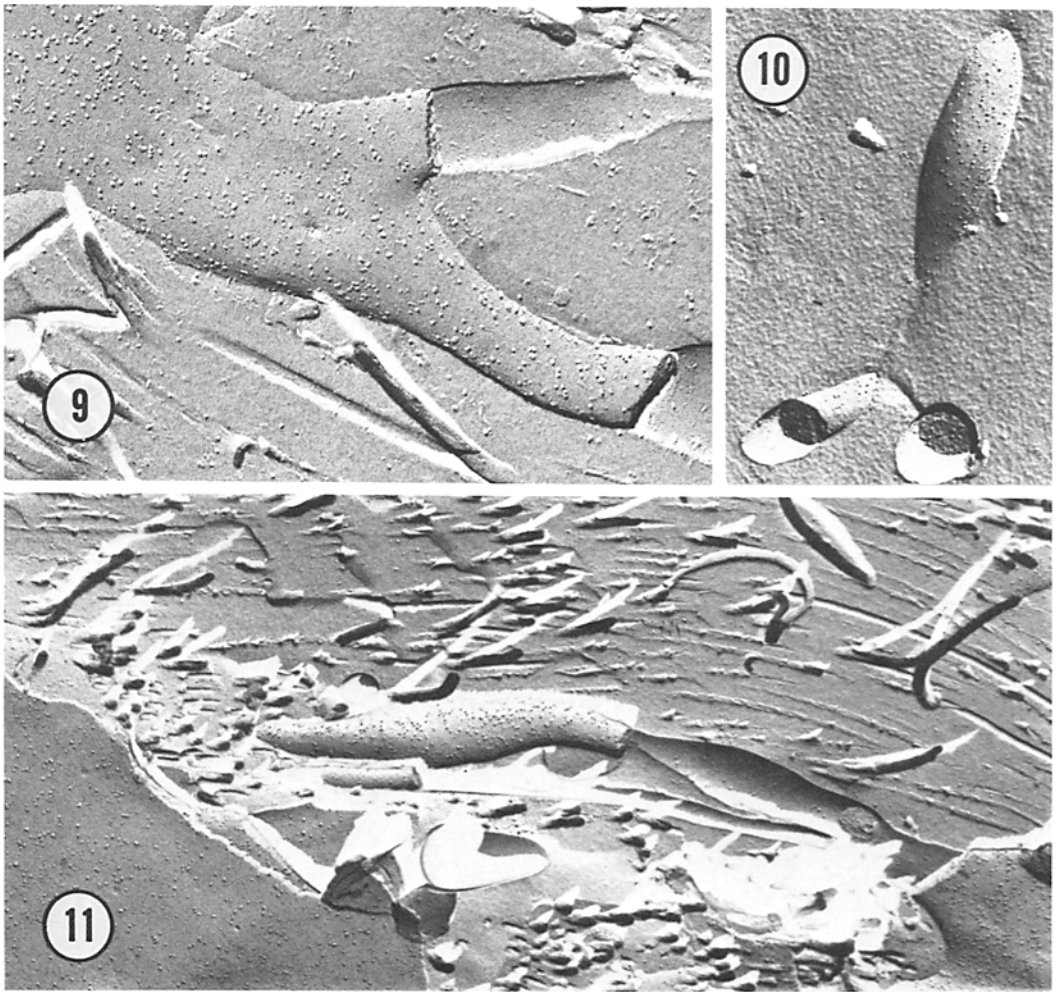

FIGURES 9–11 Electron micrographs of freeze-fracture replicas demonstrating the morphology of filopodia either next to (Figs. 9 and 11) or at some distance away from the cell body (Fig. 10). Filopodia of maturing (15 day old) fibroblasts (Fig. 9) are similar to those of young (7 day old) actively migrating fibroblasts (Figs. 10 and 11). We have seen no unique membrane architecture on filopodia. Notice that the filopodium in Fig. 11 follows the direction of the collagen fibrils. It is also evident from Fig. 11 that many of the collagen fibrils do not fracture and that their stems cast long shadows on the replica. Fig. 9, × 68,000; Fig. 10, × 39,000; Fig. 11, × 26,700.

cornea and other embryonic material. They are not seen in fractures of unfixed corneas and thus are probably artefactual.

Intercellular Junctions Between Fibroblasts

In both the migrating phase and differentiative phase of corneal morphogenesis, fibroblasts contact each other by means of the cell processes described above. In some cases, gap junctions and, even more rarely, focal tight junctions occur at these points of contact.

The typical gap junction between fibroblasts at 15 days was located between a filopodium from one cell and another cell upon the surface of which the filopodium spreads (Fig. 12). Most of the junctions observed were rather elongated in shape, suggesting that they were formed by filopodia touching each other or by a filopodium (Fig. 12) contacting the cell body of an adjacent fibroblast. Usually, the regularly packed P face IMP were separated by particle-free aisles (Fig. 13), as described for gap junctions among other types of cells (45). Junctions varied in size from a small island of 10–30 hexagonally arrayed particles to a group of islands containing up to a maximum of 2,000 IMP. Thus, the largest junctions were still relatively small; by comparison, an average gap junction between embryonic corneal epithelial cells is 5–10 times the size of the largest fibroblast gap junction.

We have not attempted to quantitate the number of fibroblast gap junctions in relation to the age of the embryo, but we have the impression that the number of junctions and the size and the packing of P face IMP within the junctions remain fairly similar from one age to the next. Since proliferation and migration cease shortly before day 15, it was especially pertinent to determine whether or not gap junctions increase in number after day 15. Freeze-fracture, however, reveals that the typical gap junctions seen between fibroblasts on day 6 (Fig. 14) are very similar in number, size and shape to those at day 15.

In addition to gap junctions, we have observed ridges on the P face (Fig. 15) that are very similar to the isolated pieces of tight junctions which Revel et al. (46) described in freeze-fracture replicas of primitive streak mesenchyme. These ridges are probably the freeze-fracture counterpart of the so-called focal tight junctions seen in thin-sections of corneal fibroblasts (21). Such junctions were infrequently observed during the first days of fibroblast migration into the stroma and have not been observed at all after day 9. No desmosomes could be observed in our micrographs of freeze-fractured fibroblasts, although desmosome-like junctions have been described between 10-day fibroblasts viewed in thin sections (21).

Changes in Intramembranous Particles (IMP)

A survey of fibroblasts of different ages immediately reveals a dramatic increase in the concentration of nonjunctional P face IMP as the age of the cornea increases (Fig. 16). To quantitate the changes in IMP concentration, we used a standard morphometric technique to estimate the number of particles per square micrometer. We found that the increase in IMP concentration from day 6 to day 19 does not occur gradually, but rather that there is a dramatic increase in P face IMP concentration over just the last few days of this period, namely, from day 15 to day 18 (Fig. 17, ●═●). Quantitative data were collected only from P faces for this study, but preliminary estimates of E face IMP concentration indicate that there is an increase on this face also, from approximately 50/μm^2 on day 6 to approximately 250/μm^2 on day 18 (Fig. 18). Interestingly, the IMP increase on the P face at 15 days is preceded by a statistically significant decrease from day 6 to day 15 (Fig. 17).

In addition to the obvious increase in IMP concentration beginning at day 15, there is an apparent change in the diversity of IMP size classes with increasing age. IMP on the P face of 6-day fibroblasts seem to be much more uniform than those of 19-day fibroblasts (Fig. 16). We have obtained quantitative information on the different size classes present at days 6 and 19 which confirm the visual impression of an apparent difference in uniformity of IMP sizes between 6- and 19-day fibroblasts (Fig. 19). The class of large IMP (12.5 nm in diameter) constitutes almost 50% of the IMP on the P face at 6 days. There is a dramatic shift to more particles of smaller diameter in the plasmalemma of older cells. It is also interesting to note that except for junctional elements described above, localized concentrations (aggregates or clumps) or IMP were not observed before day 15. However, with the increase in concentration of IMP the number of particles which appeared clumped together increased. Short, linear arrays as well as clumps were common at later ages (arrows, Fig. 16).

We performed several experiments in an at-

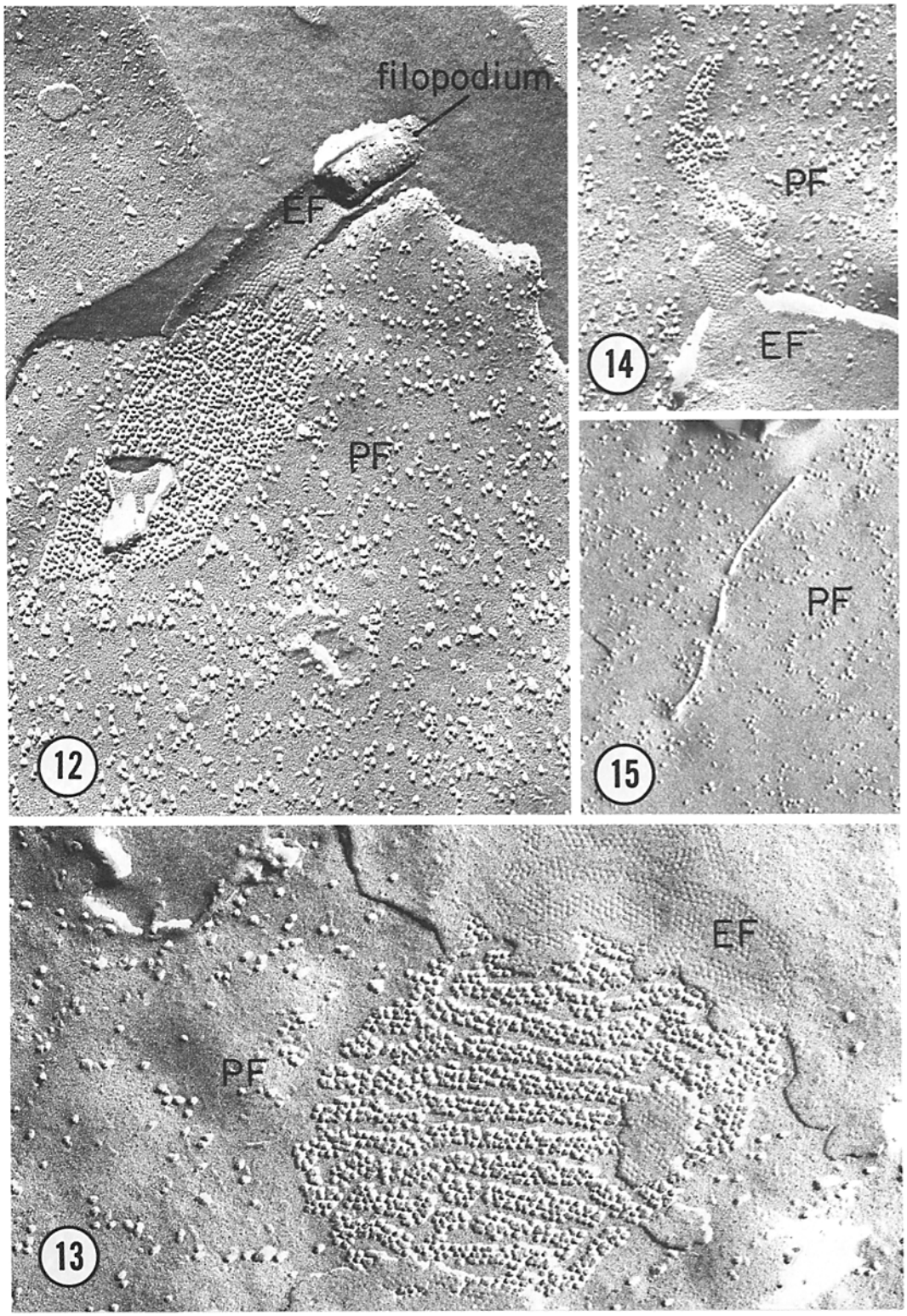

FIGURES 12–15 Electron micrographs of freeze-fractured corneal fibroblasts demonstrating gap and tight junctions. Fig. 12 shows a filopodium from a cell out of the plane of fracture which spreads out upon the surface of an adjacent fibroblast and forms a typical gap junction. Pits are seen in the E face (*EF*) of the filopodium and particles on the P face (*PF*) of the other cell. This micrograph is from a 15-day cornea. Fig. 13 demonstrates a gap junction from a 13-day fibroblast which has the particle-free aisles often found in gap junctions between these cells. Gap junctions between fibroblasts from younger corneas (Fig. 14, 6 day) look quite similar to the older junction depicted in Fig. 12. Fig. 15 (6 day) demonstrates a P face ridge which looks very much like an isolated segment of tight junction. This ridge probably represents the freeze-fracture counterpart of the so-called focal tight junction (21). Fig. 12, × 97,000; Fig. 13, × 129,600; Fig. 14, × 97,000; Fig. 15, × 83,000.

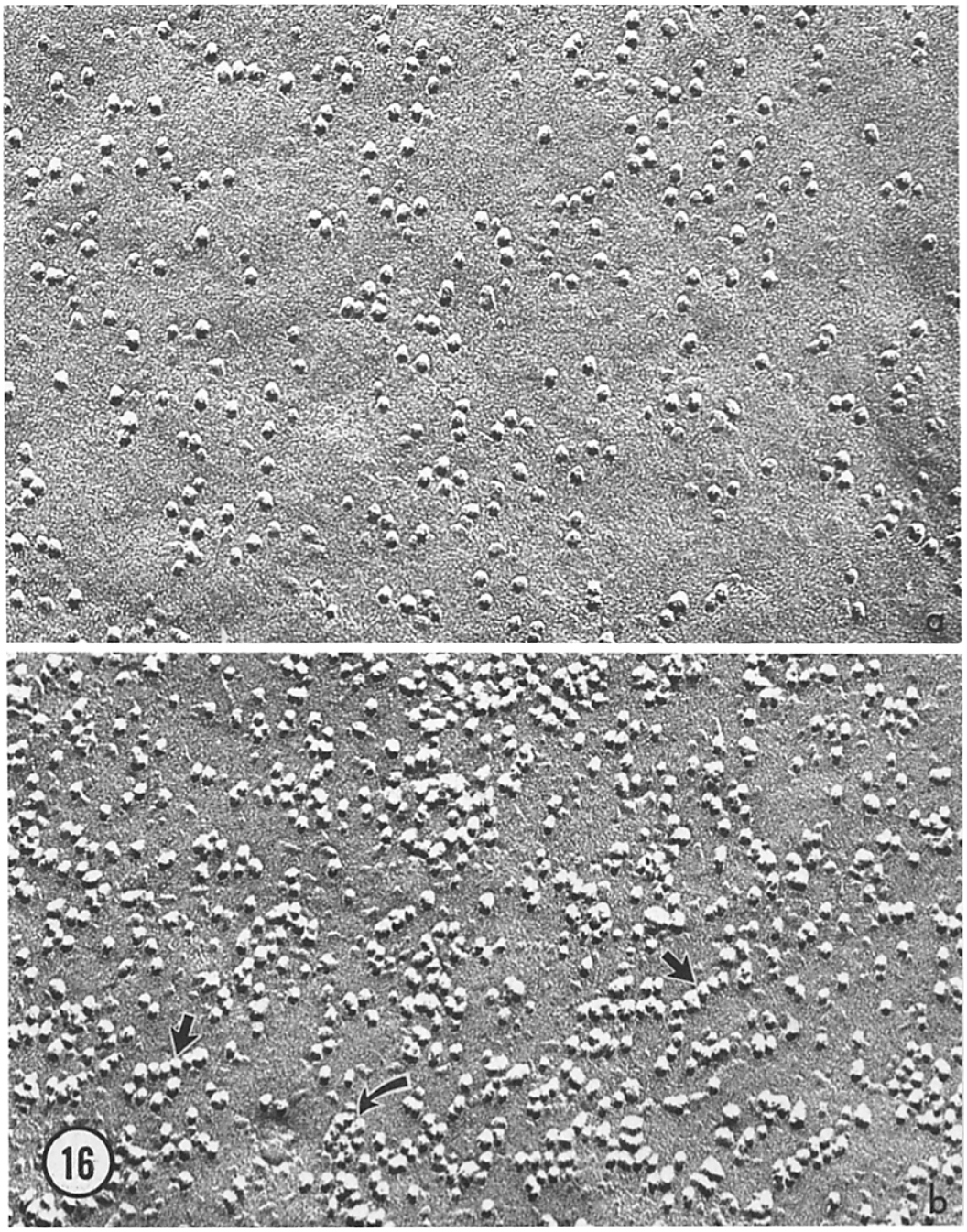

FIGURE 16 High magnification electron micrographs demonstrating the P face plasmalemma typical of 6-day (*a*) and 19-day (*b*) fibroblasts. The increase in number of IMP from 6 to 19 days is obvious. There is also an increase in the diversity of IMP size between 6 and 19 days. As the particles increase in number, linear arrays (straight arrows), and small clumps (curved arrow) become common. × 176,000.

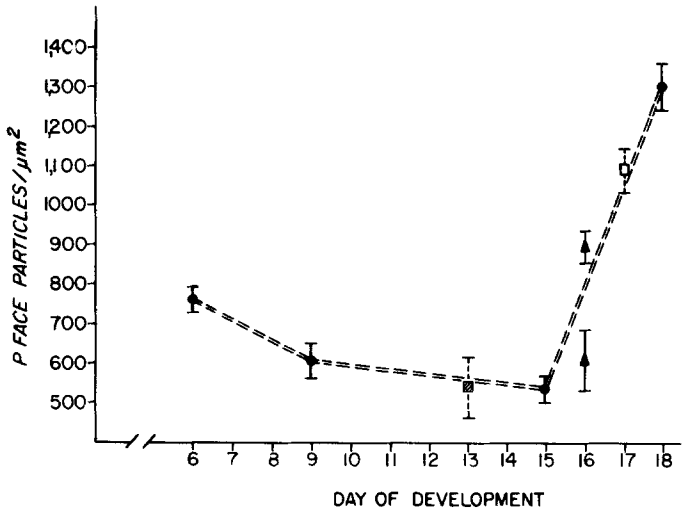

FIGURE 17 Graphic representation of morphometric analyses of P face IMP concentration during normal corneal development and after thyroxine or thiouracil treatment. Normally, the IMP concentration of the fibroblast plasmalemma decreases gradually, from 760 ± 20/μm^2 on day 6 to 534 ± 70/μm^2 on day 15, before the dramatic jump to 1300 ± 45/μm^2 on day 18 (●═●). At 16 days, when the posterior half of the cornea has condensed (Fig. 1), the IMP concentration of flattened fibroblasts in the posterior half rises to 895 ± 24/μm^2 (▲) while that of the rounded fibroblasts in the anterior half is only 602 ± 60/μm^2 (▲). Thyroxine treatment from day 11 to day 13 speeds up the process of condensation (Fig. 21), but the IMP concentration of the fibroblasts in thyroxine-treated corneas on day 13 is 545 ± 70/μm^2 (▨), exactly the concentration of an untreated control at that age. Thiouracil treatment from day 9 prevents condensation at day 17 (Fig. 21), but the IMP concentration of these fibroblasts at 17 days is 1088 ± 40/μm^2 (□). Thus, neither treatment had any effect on the IMP concentration of corneal fibroblasts.

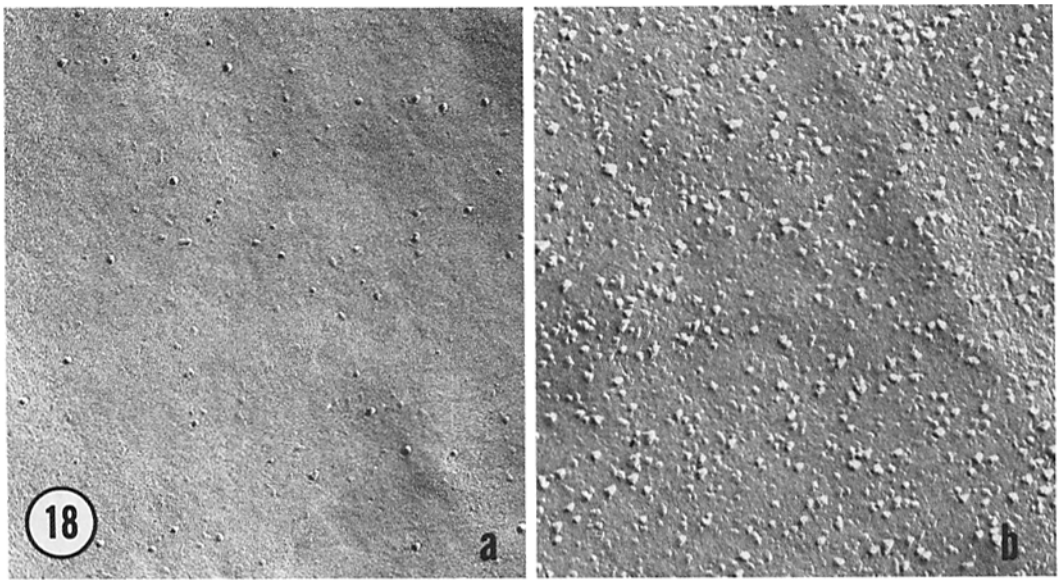

FIGURE 18 High magnification electron micrograph demonstrating the E face plasmalemma typical of 6-day (*a*) and 19-day (*b*) fibroblasts. × 85,200.

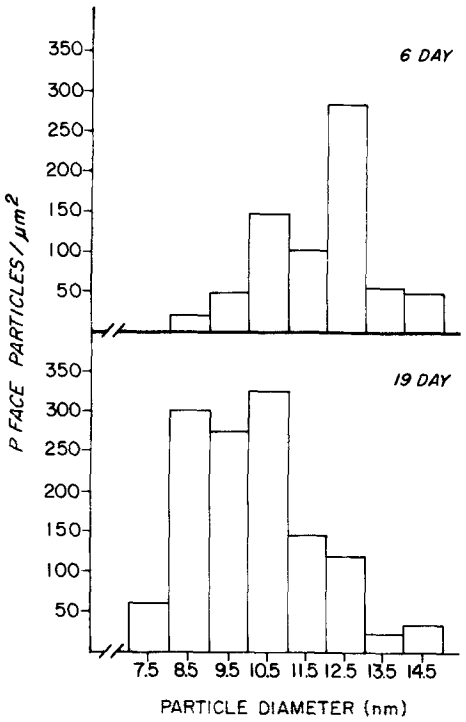

FIGURE 19 Bar graphs showing the size of P face IMP for 6- and 19-day corneal fibroblasts. IMP diameter was measured as the width of the shadow cap perpendicular to the direction of shadowing. The particles were grouped into 1-nm size classes from 7.5 to 14.5 nm. At 6 days, the particles are larger and most are 10.5–12.5 nm in diameter. At 19 days, there is a noticeable shift to smaller particles, some as small as 7.5 nm in diameter.

tempt to judge whether or not the chronology of the dramatic increase in IMP concentration between day 15 and day 18 is related to any of the known physiological changes taking place in the cornea at this time. First, we evaluated collagen and GAG synthesis per cornea from day 14 to day 19 to determine whether the IMP increase parallels increased synthetic activity of the fibroblasts. The epithelium and endothelium were surgically removed and, since there is no further fibroblast proliferation after day 14, the values per cornea represent synthesis by the same number of fibroblasts at each stage (Fig. 20). Our results confirm and extend those of Coleman et al. (10) and of Conrad (11). Collagen synthesis increases until day 16 and then begins to decline. GAG synthesis increases from day 14 to day 19 (Fig. 20). In the adult chicken cornea, collagen synthesis drops to about 10% of the value at 16 days. GAG production in the adult is on the order of 50% of the GAG value at 16 days. Preliminary estimates of IMP concentration in adult fibroblasts indicate that the particle count remains elevated (~1,000/μm^2). Thus, there is no obvious relation between IMP number and fibroblast synthetic activity.

To determine whether or not the IMP increase is related to the process of stromal condensation, we obtained replicas from corneas of 16 days which were fractured through either the condensed (posterior) or the noncondensed (anterior) portions of the stroma (see 15 days, Fig. 1). This experiment initially suggested that the IMP concentration increase might be caused by some factor involved in condensation, for we found two distinct populations of cells in the two parts of the stroma with respect to their IMP concentration (Fig. 17; 16 days, ▲). The increased IMP in the plasmalemma of posterior, flattened fibroblast (Fig. 2*b*) as compared with the anterior, rounded fibroblast (Fig. 2*a*) is not due to the change in cell shape *per se*. A two-dimensional morphometric test showed that the membrane perimeter/cytoplasmic area ratio of 14- and 19-day fibroblasts is quite similar (Table I), indicating that no major alteration in membrane area per cell occurs at this time.

Since the most important factor that is causally linked to the condensation is thyroxine, we next injected embryos with thyroxine to speed up or thiouracil to slow down condensation to see whether the IMP increase would occur prematurely in the former case or be delayed in the latter. Embryos were injected with thyroxine on day 11 and sacrificed 2 days later, on day 13. Thiouracil-treated embryos were injected on day 9 and sacrificed 8 days later, on day 17. The effectiveness of these treatments in accelerating or delaying the process of condensation (13, 29) is demonstrated in Figure 21.

Counts of P face IMP demonstrate that the concentration did not increase prematurely when stroma condensation was induced early by thyroxine treatment (Fig. 17; 13 days, ▨). These results suggest that the IMP increase which occurs between days 15 and 18 is not due to stromal condensation, since premature condensation does not cause premature particle proliferation. This interpretation was confirmed by the results from thiouracil-treated embryos. In this case, the IMP concentration of corneal fibroblasts increased even though condensation failed to occur (Fig. 17; 17 days, □). Thus, the only parameter to which the IMP increase is clearly related is the age of the

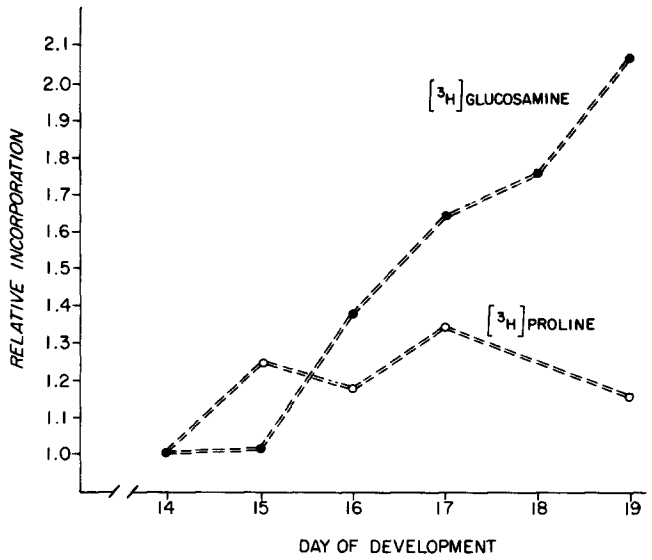

FIGURE 20 Graph showing the incorporation of [^{3}H]glucosamine into GAG and of [^{3}H]proline into collagen by corneal fibroblasts. The epithelium and endothelium were surgically removed and the fibroblast-rich stroma was incubated with the appropriate isotope for 4 h at 37°C. GAG synthesis increases throughout the period studied, while collagen synthesis increases through day 17 and then begins to decline. Each point is the mean for 10 determinations (4 stromas each).

fibroblast in terms of time spent in the cornea. The posterior fibroblast (Fig. 2*b*) entered the primary corneal stroma first and resided longer in the ECM created by the epithelium than the anterior fibroblast (Fig. 2*a*).

DISCUSSION

Between the time of their entry into the domain of the primary corneal stroma on day 6 and day 18 or 19 of incubation, by which time the cornea has taken on its mature form, the fibroblasts pass through several phases in their differentiation. In this study, we have described the principal features of corneal fibroblasts and the adjacent extracellular matrix revealed by the freeze-fracture and freeze-etch techniques, with emphasis on the changes in plasmalemma ultrastructure which occur during cytodifferentiation. The possible morphogenetic implications of these findings will be considered in the discussion.

Fibroblast cell processes of various sizes and shapes corresponding to filopodia and lamellipodia (4) were readily identified at each age studied. During early stages, when the cells are still actively migrating, these cell processes were observed to extend from the cell, to form attachments to the substratum and to contract (4). Considerable effort has been made in the past to discern how cells adhere to their substratum, but very little is known about the nature of such adhesions (43). We had anticipated that the freeze-fracture technique might reveal some indication of plasmalemma specialization, such as a unique arrangement of particles on filopodia, but none was observed. Moreover, the particle distribution and concentra-

TABLE I

Morphometric Analysis of Fibroblast Shape Changes

Age	N*	Cytoplasmic area	Membrane perimeter length	Membrane/cytoplasm ratio
		$\mu m^2/100\ \mu m^2$	$\mu m^2/100\ \mu m^2$	
14 days	21	13.6 ± 1.4	53 ± 8.2	1.35
19 days	14	15.3 ± 1.2	90 ± 13.3	2.0‡

* N is the number of micrographs counted; there were usually 2-5 nuclei included per micrograph at × 15,000 magnification. Values for area and perimeter appearing in the micrographs are reported as mean ± SEM.

‡ The fact that the plasmalemma area increases at 19 days as compared to 14 days indicates that a decrease in membrane area per cell does not cause the observed concentration of IMP (Fig. 16). The cell number is constant during the period illustrated and the cell shape at 19 days is actually flatter than at 14 days, as these data suggest.

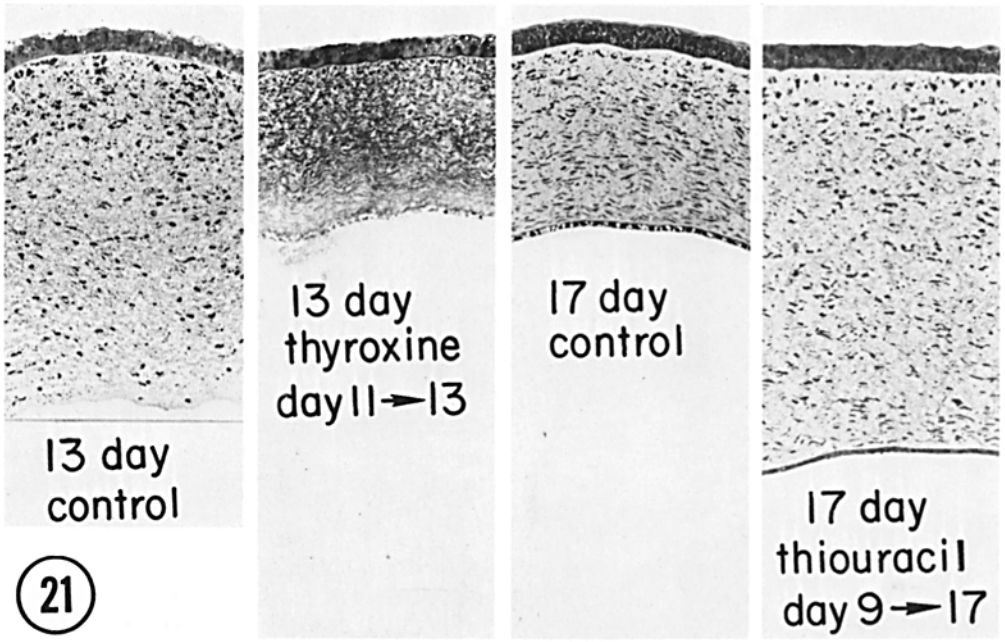

FIGURE 21 Light micrographs demonstrating the effects of thyroxine and thiouracil treatment on stromal condensation. The 13-day control cornea shows no condensation. After thyroxine treatment from day 11 to day 13, two-thirds of the cornea is condensed at day 13, the stromal width is greatly reduced, and there are many layers of flattened cells. The appearance of a 17-day control cornea is very similar to that of the 13-day thyroxine-treated cornea. The 17-day cornea treated with thiouracil from day 9 to day 17, however, is very similar to the 13-day control; little or no condensation has occurred. × 216.

tion on filopodia was similar to that on cell bodies at any given age.

The fact that the IMP concentration and distribution on filopodia was not different from that of the cell body may have a bearing on our understanding of membrane formation. This observation suggests that fibroblast filopodia might be formed either by extending a specific portion of preformed plasmalemma, with IMP being already present, or by adding new membrane at the tip of an elongating process with the appropriate integral proteins (IMP) being inserted simultaneously with the lipid components. This is in contrast to the apparent mode of growth of axonal processes of neurons reported by Pfenninger and Bunge (38). Since the plasmalemma of the tip of growing axonal processes has a much lower particle number than proximal plasmalemma, they suggested that growth at the tip might be due to the insertion of new, particle-free membrane from particle-free cytoplasmic vesicles found in the growth cone (38). "Maturation" of new axonal membrane seems to be accompanied by the appearance of particles, which could be added either by insertion directly into the membrane at these distal points or by lateral movement within the membrane. The intensity of ferritin-conjugated lectin staining of the neuronal surface coat is uniform, however, even on the growth cone, and so does not parallel the arrangement of IMP (39). Nerve axon elongation differs from migratory cell locomotion in several respects (27). It is tempting to suggest that the more usual mechanism of cell process formation may be to insert lipid and IMP simultaneously, as our observations imply, rather than to insert the lipid first.

A chronological survey of general fibroblast plasmalemma ultrastructure revealed several changes in IMP concentration and heterogeneity in the plasmalemma of cell bodies and cell processes between 6 and 19 days. In this period, there is a gradual increase in diversity of IMP size. With time, more small particles are intermixed with the original IMP class. This change is not related to IMP concentration. In fact, there is a decrease in IMP between day 6 and day 14 (from 760 μm^2 to 534 μm^2) and an increase from day 15 to day 18 (from 534 μm^2 to 1,300 μm^2). The decrease oc-

curs during the period in which proliferation slows and migration ceases. Scott et al. (48) report a severalfold decrease in IMP concentration at mitosis, but a return to premitotic levels within a few hours in synchronously dividing cells. Therefore, there is little reason to believe that cessation of proliferation would result in an overall decrease in IMP concentration. The changes in IMP concentration do not parallel fibroblast anabolism, either. Fibroblast synthetic machinery and productivity increase throughout the period, without relation to IMP concentration, and when collagen and GAG synthesis drop later on, IMP concentration shows no significant change.

The dramatic event that begins at 14–15 days, when the gradual decrease in IMP concentration suddenly shifts to a rapid increase, is stroma condensation. Water is pumped out of the cornea, hyaluronate disappears presumably by enzymatic digestion, chondroitin and keratan sulfate become the principal GAG, and the cornea becomes transparent (11, 12, 21, 52). As condensation proceeds, the entrapped fibroblasts assume the sessile, flattened form characteristic of the mature cornea. Thus, our working hypothesis seemed obvious: some factor involved in stromal condensation might be stimulating the increase in plasmalemma IMP concentration.

The hypothesis at first seemed to stand. We analyzed the plasmalemma of cells in both the condensed and the noncondensed parts of the corneal stroma at 16 days and we found that these two populations of corneal fibroblasts are, indeed, different with regard to IMP concentration. Flattened fibroblasts in the posterior, condensed zone have twice the concentration of IMP as do the round or elongate fibroblasts in the anterior, uncondensed zone.

Coulombre and Coulombre (13) and Masterson et al. (29) have shown that corneal stroma condensation is initiated by thyroxine, presumably through activation of endothelial solute transport. Thus, it is possible to inhibit condensation by treating embryos with thiouracil or to initiate premature condensation with thyroxine. Freeze-fracture and morphometric analysis of the plasmalemma of thyroxine- and thiouracil-treated corneas indicated that neither treatment affected the normal sequence of changes in IMP concentration. The IMP increase occurred in the absence of stromal condensation and fibroblast flattening when embryos were treated with thiouracil and failed to be induced early by thyroxine treatment, even though the stroma condensed precociously.

Therefore, although the membrane particle increase proceeds from posteriorly located cells to anterior cells, it is not caused by stromal condensation or by flattening of the cells. Nor is it due to any direct effect of thyroxine. Indeed, it seems to be independent of all processes which we know are occurring in the cornea at this time, except age-dependent maturation. The fibroblasts in the posterior cornea entered the cornea first and began their cytodifferentiation sooner. The possibility that this membrane maturation is a process inherent in the differentiation of mesenchymal cells once they have entered the fibroblast pathway is suggested by preliminary evidence showing a similar change in membrane particle concentration in tendon fibroblast plasma membrane over this same period.

A review of studies that have been done to date on other developing cells supports the idea that an increase in the number of IMP, and probably also in diversity, would be expected as cells mature. The number of particles reported in freeze-cleave studies of young versus more mature cells is of the same order of magnitude as the overall change (534 μm^2 to 1,300 μm^2) we report here between 14 and 19 days in the chick cornea. The P face IMP concentration of sarcoplasmic reticulum (SR) from embryonic chick muscle increases from 406/μm^2 on day 14 of development to 672/μ^2 on day 18 of development, and then to 3,853/μm^2 on day 25 after hatching (50). During this period the plasmalemma P face IMP concentration increased from 165/μm^2 to 269/μm^2, and then to 403/μm^2 by 42 days after hatching (50). The increase in IMP of the SR parallels an increase in the activity of the SR calcium pump (6). The plasmalemma of fetal rat neurons developing in vivo increases from 112/μm^2 to 743/μm^2 between day 15 and day 17, while the IMP concentration of similar cells explanted at day 15 and maintained in vitro first drops to 53/μm^2 at 5 days of culture and then increases to 527/μm^2 by day 40 of culture (38). Other evidence for membrane maturation comes from studies indicating the appearance of new membrane antigens during differentiation (3, 5, 16), but there is, as yet, no evidence linking the new antigens with IMP changes.

In addition to the general cell membrane IMP discussed above, all of these cells can exhibit localized concentrations of IMP in the form of tight junctions and gap junctions. The fact that mesenchymal cells (46, 54) and fibroblast-like

cells (41, 42, 45) have gap junctions is not widely appreciated due to the preponderance of the work on junctional complexes between epithelial cells. The corneal fibroblasts are united by perfectly typical gap junctions which are not as extensive as those in their epithelial neighbors but which, nevertheless, are striking as viewed in freeze-fractures. The few tight junctions observed do not seem to persist in the cornea and thus may be remnants from the epithelial precursors of the mesenchymal cells (46). Although it is possible that gap junctions are also remnants from epithelial ancestors, gap junctions are present at much later stages of development than the focal tight junctions, at least as late as day 18. It is tempting to believe that such junctions have a role in cell-cell communication (41, 45) in the embryonic mesenchyme.

A final point deserving brief discussion is the structure of the external membrane surface. Examination of freeze-etched replicas revealed this surface of the corneal fibroblast to be relatively smooth, in contrast to the IMP-studded fracture faces. Some extracellular material was observed in etched preparations to be arranged in the form of knobs on the outer surface of corneal fibroblasts. These knobs sometimes appear to give rise to filaments that extend to collagen fibrils, to other cells or to filaments that interconnect to form meshworks in the extracellular space. These structures, the knobs and filaments, bear a striking resemblance to punctate deposits of GAG on plasma membranes and in the ECM and to the filamentous structures connecting such particles as revealed in various tissues by ruthenium red staining (20, 25, 34, 55). There are several lines of evidence which suggest that ECM components may be involved in stabilization and/or modulation of the differentiated state (19, 23, 26, 35, 36). It will be of interest to analyze ECM-plasmalemma interaction in more detail in the future, using freeze-etching with correlated histochemical and biochemical approaches.

It is a pleasure to acknowledge the indispensable technical and intellectual assistance of Dr. D. A. Goodenough in this study. Kathleen Kiehnau's help in the biochemical analyses is also gratefully acknowledged.

This work was supported by U. S. Public Health Service grants HD-00143 and 5T01 GM00406.

Received for publication 17 August 1976, and in revised form 19 November 1976.

REFERENCES

1. ALBERTINI, D. F., D. W. FAWCETT, and P. J. OLDS. 1975. Morphological variations in gap junctions of ovarian granulosa cells. *Tissue Cell.* **7**:389-405.
2. ALBRECHT-BUEHLER, G. 1976. Filopodia of spreading 3T3 cells. Do they have a substrate-exploring function? *J. Cell Biol.* **69**:275-286.
3. BALLARD, P. L., and G. M. TOMKINS. 1970. Glucocorticoid-induced alteration of the surface membrane of cultured hepatoma cells. *J. Cell Biol.* **47**:222-234.
4. BARD, J. B. L., and E. D. HAY. 1975. The behavior of fibroblasts from the developing avian cornea. Morphology and movement *in situ* and in vitro. *J. Cell Biol.* **67**:400-418.
5. BLANCHET, J. P. 1976. The chick erythrocyte membrane antigens: Characterization and variation during embryonic and postembryonic development. *Dev. Biol.* **48**:411-420.
6. BOLAND, R., A. MARTONOSI, and T. W. TILLACK. 1974. Developmental changes in the composition and function of sarcoplasmic reticulum. *J. Biol. Chem.* **249**:612-623.
7. BRANTON, D., S. BULLIVANT, N. B. GILULA, M. J. KARNOVSKY, H. MOOR, K. MÜHLETHALER, D. H. NORTHCOTE, L. PACKER, B. SATIR, P. SATIR, V. SPETH, L. A. STAEHELIN, R. L. STEERE, and R. S. WEINSTEIN. 1975. Freeze-etching nomenclature. *Science (Wash.).* **190**:54-56.
8. BRANTON, D., and D. DEAMER. 1972. Membrane Structure. *Protoplasmatologia.* II/E/**1**:1-70.
9. CHALCROFT, J. P., and S. BULLIVANT. 1970. An interpretation of liver cell membrane and junction structure based on observation of freeze-fracture replicas of both sides of the fracture. *J. Cell Biol.* **47**:49-60.
10. COLEMAN, J., H. HERRMANN, and B. BESS. 1965. Biosynthesis of collagen and non-collagen protein during development of the chick cornea. *J. Cell Biol.* **25**:69-78.
11. CONRAD, G. W. 1970. Collagen and mucopolysaccharide biosynthesis in the developing chick cornea. *Dev. Biol.* **21**:292-317.
12. COULOMBRE, A. J., and J. L. COULOMBRE. 1958. Corneal development. I. Corneal transparency. *J. Cell Comp. Phys.* **51**:1-11.
13. COULOMBRE, A. J., and J. L. COULOMBRE. 1964. Corneal development. III. The role of the thyroid in dehydration and the development of transparency. *Exp. Eye Res.* **3**:105-114.
14. DODSON, J. W., and E. D. HAY. 1971. Secretion of collagenous stroma by isolated epithelium grown in vitro. *Exp. Cell Res.* **65**:215-220.
15. DREIFUSS, J. J., K. AKERT, C. SANDRI, and H. MOOR. 1976. Specific arrangements of membrane particles at sites of exo-endocytosis in the freeze-

etched neurohypophysis. *Cell Tissue Res.* **165:**317–325.
16. GOLDSCHNEIDER, I. 1974. Surface antigens and differentiation of thymus-dependent lymphocytes. *In* The Cell Surface in Development. A. A. Moscona, editor. John Wiley and Sons, New York.
17. GOODENOUGH, D. A., and J. P. REVEL. 1970. A fine structural analysis of intercellular junctions in the mouse liver. *J. Cell Biol.* **45:**272–290.
18. HAMILTON, H. L. 1952. Lillie's Development of the Chick. An introduction to embryology. Holt, Rinehart and Winston, Inc., New York.
19. HAY, E. D. 1973. Origin and role of collagen in the embryo. *Amer. Zool.* **13:**1085–1107.
20. HAY, E. D., and S. MEIER. 1974. Glycosaminoglycan synthesis by embryonic inductors: Neural tube, notochord and lens. *J. Cell Biol.* **62:**889–898.
21. HAY, E. D., and J. P. REVEL. 1969. Fine Structure of the Developing Avian Cornea. S. Karger AG, Basel.
22. HONG, K., and W. L. HUBBELL. 1972. Preparation and properties of phospholipid bilayers containing rhodopsin. *Proc. Natl. Acad. Sci. U.S.A.* **69:**2617–2621.
23. HUANG, D. 1974. Effect of extracellular chondroitin sulfate on cultured chondrocytes. *J. Cell Biol.* **62:**881–886.
24. JOHNSTON, M. C., A. BHAKDINARONK, and Y. C. REID. 1974. An expanded role of the neural crest in oral and pharyngeal development. *In* Oral Sensation and Perception – Development in the Fetus and Infant. J. F. Bosma, editor. U. S. Government Printing Office, Washington, D. C.
25. KELLEY, R. O. 1975. Ultrastructural identification of extracellular matrix and cell surface components during limb morphogenesis in man. *J. Embryol. Exp. Morphol.* **34:**1–18.
26. KONIGSBERG, I. R., and S. D. HAUSCHKA. 1965. Cell and tissue interactions in the reproduction of cell type. *In* Reproduction: Molecular, Subcellular and Cellular. M. Locke, editor. Academic Press Inc., New York.
27. LETOURNEAU, P. C., and N. K. WESSELLS. 1974. Migratory cell locomotion versus nerve axon elongation. Differences based on the effects of lanthanum ion. *J. Cell Biol.* **61:**50–69.
28. MARCHESI, V. T., T. W. TILLACK, R. L. JACKSON, J. P. SEGREST, and R. E. SCOTT. 1972. Chemical characterization and surface orientation of the major glycoprotein of the human erythrocyte membrane. *Proc. Natl. Acad. Sci. U.S.A.* **69:**1445–1449.
29. MASTERSON, E., H. F. EDELHAUSER, and D. L. VAN HORN. 1975. Development of corneal transparency in embryonic chick: Influence of exogenous thyroxine and thiouracil on structure, water and electrolyte content. *Dev. Biol.* **43:**233–239.
30. MCNUTT, N. S., and R. S. WEINSTEIN. 1973. Membrane ultrastructure at mammalian intercellular junctions. *Prog. Biophys. Mol. Biol.* **26:**45–101.
31. MEIER, S. and E. D. HAY. 1973. Synthesis of sulfated glycosaminoglycans by embryonic corneal epithelium. *Dev. Biol.* **35:**318–331.
32. MEIER, S., and E. D. HAY. 1974. Control of corneal differentiation by extracellular materials. Collagen as a promoter and stabilizer of epithelial stroma production. *Dev. Biol.* **38:**249–270.
33. MISRA, D. N., and N. N. DAS GUPTA. 1966. Distortion in dimensions produced by shadowing for electron microscopy. *J. R. Microsc. Soc.* **84:**373–384.
34. MYERS, D. B., T. C. HIGHTON, and D. G. RAYNS. 1973. Ruthenium red-positive filaments interconnecting collagen fibrils. *J. Ultrastruct. Res.* **42:**87–92.
35. NEVO, Z., and A. DORFMAN. 1972. Stimulation of chondromucoprotein synthesis in chondrocytes by extracellular chondromucoprotein. *Proc. Natl. Acad. Sci. U. S. A.* **69:**2969–2972.
36. NEWSOME, D. A. 1976. In vitro stimulation of cartilage in embryonic chick neural crest cells by products of retinal pigmented epithelium. *Dev. Biol.* **49:**496–507.
37. NICOLSON, G. L. 1976. Transmembrane control of the receptors on normal and tumor cells. I. Cytoplasmic influence over cell surface components. *Biochim. Biophys. Acta.* **457:**57–108.
38. PFENNINGER, K. H., and R. P. BUNGE. 1974. Freeze-fracturing of nerve growth cones and young fibers. A study of developing plasma membrane. *J. Cell Biol.* **63:**180–196.
39. PFENNINGER, K. H., and M.-F. MAYLIÉ-PFENNINGER. 1975. Distribution and fate of lectin binding sites on the surface of growing neuronal processes. *J. Cell Biol.* **67:**332a.
40. PINTO DA SILVA, P., and D. BRANTON. 1970. Membrane splitting in freeze-etching; covalently bound ferritin as a membrane marker. *J. Cell Biol.* **45:**598–605.
41. PINTO DA SILVA, P., and N. B. GILULA. 1972. Gap junctions in normal and transformed fibroblasts in culture. *Exp. Cell Res.* **71:**393–401.
42. PINTO DA SILVA, P., and A. MARTINEZ-PALOMO. 1975. Distribution of membrane particles and gap junctions in normal and transformed 3T3 cells studied *in situ*, in suspension and treated with concanavalin A. *Proc. Natl. Acad. Sci. U.S.A.* **72:**572–576.
43. PORTER, R., and D. W. FITZSIMONS. 1973. Locomotion of Tissue Cells. Associated Scientific Publishers, New York.
44. RAYNS, D. G. 1974. Collagen from frozen fractured glycerinated beef heart. *J. Ultrastruct. Res.* **48:**59–66.

45. REVEL, J. P., A. G. YEE, and A. J. HUDSPETH. 1971. Gap junctions between electrotonically coupled cells in tissue culture and in brown fat. *Proc. Natl. Acad. Sci. U.S.A.* **68**:2924–2927.
46. REVEL, J. P., P. YIP, and L. L. CHANG. 1973. Cell junctions in the early chick embryo—A freeze-etch study. *Dev. Biol.* **35**:302–317.
47. RUBEN, G. C., J. N. TELFORD, and R. C. CARROLL. 1976. Identification and transmembranous localization of active cytochrome oxidase in reconstituted membranes of purified phospholipids by electron microscopy. *J. Cell Biol.* **68**:724–739.
48. SCOTT, R. E., R. L. CARTER, and W. R. KIDWELL. 1971. Structural changes in membranes of synchronized cells demonstrated by freeze-cleavage. *Nature* (*Lond.*). **233**:219–220.
49. SWEENEY, B. M. 1976. Freeze-fracture studies of the thecal membranes of *Gonyaulax polyhedra:* Circadian changes in the particles of one membrane face. *J. Cell Biol.* **68**:451–461.
50. TILLACK, T. W., R. BOLAND, and A. MARTONOSI. 1974. The ultrastructure of developing sarcoplasmic reticulum. *J. Biol. Chem.* **249**:624–633.
51. TILLACK, T. W., and V. T. MARCHESI. 1970. Demonstration of the outer surface of freeze-etched red blood cell membranes. *J. Cell Biol.* **45**:469–473.
52. TOOLE, B. P., and R. L. TRELSTAD. 1971. Hyaluronate production and removal during corneal development in the chick. *Dev. Biol.* **26**:18–35.
53. TORRES-PEREIRA, J., R. MEHLHORN, A. D. KEITH, and L. PACKER. 1974. Changes in membrane lipid structure of illuminated chloroplasts—Studies with spin-labeled and freeze-fractured membranes. *Arch. Biochem. Biophys.* **160**:90–99.
54. TRELSTAD, R. L., E. D. HAY, and J. P. REVEL. 1967. Cell contact during early morphogenesis in the chick embryo. *Dev. Biol.* **16**:78–106.
55. TRELSTAD, R. L., K. HAYASHI, and B. P. TOOLE. 1974. Epithelial collagens and glycosaminoglycans in the embryonic cornea. Macromolecular order and morphogenesis in the basement membrane. *J. Cell Biol.* **62**:815–830.